*Scientific Journal of Riga Technical University*
Construction Science

*2010*

*Volume 11*

# Non-Uniform Distribution of Moisture Influence on Shape of Plywood Sheet

Janis Sliseris, *Riga Technical University*, Karlis Rocens, *Riga Technical University*

***Abstract:*** **Moisture distribution through the thickness of plywood is analyzed when the sheet is subjected to different relative air humidity from both sides using one dimensional diffusion equation. The shape change of plywood sheet is numerically analyzed when moisture influence from both sides of sheet is not time – dependent, and also when one side of the sheet is subjected to time-dependent outside moisture-temperature conditions and conditions on other side is not time-dependent. The outdoor moisture-temperature conditions were taken form national standard LBN-003-01 "Būvklimatoloģija" and approximated with third order polynomial using its average values summed with average amplitude.**

***Keywords:*** **bound water diffusion, plywood sheet, curvature of sheet, geometrical nonlinearity**

## I. INTRODUCTION

Composite sheets with multilayer structure are widely used as load bearing constructions. One of the most popular is plywood sheets that are made from birch veneers. Thin veneers that are made by rotary cut log of birch can be assumed as orthotropic material. Typically composite sheets are made with odd number of veneers with symmetrical structure in respect to mid-surface of the sheet, for example 7-layer or 9-layer structure.

There are many environmental actions which influence behaviour of load bearing sheets. The sheets that are made from wood veneers are significantly affected by air moisture. Usually environmental conditions in both sides of the sheet are not the same. The environment could differ with temperature, air moisture, pressure conditions and others. As a result of different conditions of air moisture and temperature from each side of the sheet the moisture content and temperature of the sheet changes through its thickness. Mathematically it could be described with system of mass and heat transfer equation [1], [2]. In isothermal case moisture diffusion could be modelled by Fick`s second law [3]-[6]. As a result of moisture gradient through the thickness of the sheet it obtains asymmetrical structure with respect to its mid surface and changes initial shape. The flat sheet becomes curved in two directions and as well as linear dimension change, in some cases it warps.

## II. MOISTURE DIFFUSION

The bound water diffusion in wooden veneer could be modelled by Fick's 2. law [5] (if moisture content is below fibre saturation point (FSP)):

$$\frac{\partial m(Z,t)}{\partial t} = \frac{\partial}{\partial Z}\left(D\big(m(Z,t),T\big)\frac{\partial m(Z,t)}{\partial Z}\right),\ -a < Z < a,\quad t > 0 \quad , \qquad (1)$$

where

m- moisture content of wood (kg/kg);

$D(m(Z,t),T)-$bound water diffusion coefficient (m$^2$/h), according to [6] for Red oak (assumed to be the same for birch tree) it is

$$D(m(Z,t),T) = 5.76\cdot\exp\left(1.45\cdot m(Z,t) - \frac{5280}{T}\right), \qquad (2)$$

where

*t*- time (h);

*T*- temperature (K);

*a*- half of thickness of the sheet;

*Z*- coordinate with zero value at mid surface of the sheet, on axis orthogonally to sheet surface .

The initial condition of partial differential Eq. (1) is

$$m(Z,0) = m_0\,, \qquad (3)$$

and boundary conditions are

$$D(m(Z,t),T)\frac{\partial m(Z,t)}{\partial Z} = k_m\,(m(Z,t) - m_0),\ Z = \pm a\ t > 0 \quad , \qquad (4)$$

where

$k_m -$surface emission coefficient (m/s), according to [5] in radial direction of wood it is 0.00243(m/h) for Scot pine, assumed to be the same for birch tree.

## III. DISPLACEMENT ANALYSIS

### A. Small displacement analysis

Analytical analysis of mid surface deformations, curvatures and torsion could be done be method described in [7]-[9]. In the theory of thin composite multilayer sheets it is beneficial to replace stress field with equal system of forces and moments. The relationship between the system of force and moments and strains of mid surface- $\varepsilon_X^0, \varepsilon_Y^0, \gamma_{XY}^0$ and curvatures $k_X^0, k_Y^0$ and torsion $k_{XY}^0$are shown in eq.(5). Geometrical interpretation of curvatures is shown in Fig.1.

From eq. (5) it is possible to calculate strains, curvatures and torsion if the system of forces and moments are known.

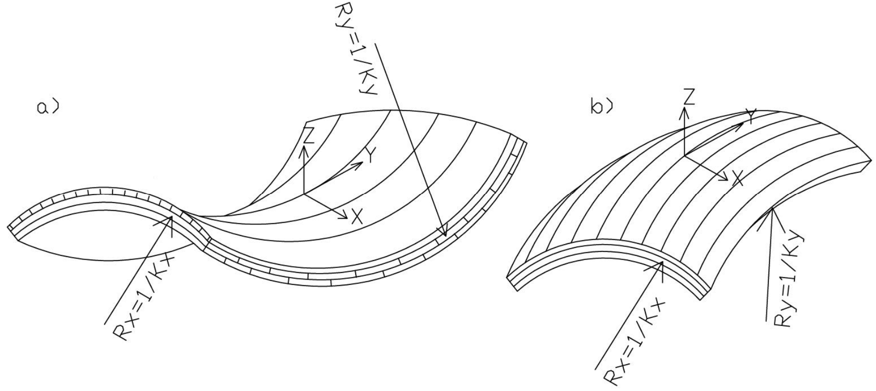

Fig. 1. Geometrical interpretation of curvature, a-negative Gaussian curvature, b- positive Gaussian curvature

$$\begin{cases} N_X^0 = A_{11}\varepsilon_x^0 + A_{12}\varepsilon_y^0 + A_{13}\gamma_{xy} + B_{11}k_X^0 + B_{12}k_Y^0 + B_{13}k_{XY}^0 \\ N_Y^0 = A_{21}\varepsilon_x^0 + A_{22}\varepsilon_y^0 + A_{23}\gamma_{xy} + B_{21}k_X^0 + B_{22}k_Y^0 + B_{23}k_{XY}^0 \\ N_{XY}^0 = A_{31}\varepsilon_x^0 + A_{32}\varepsilon_y^0 + A_{33}\gamma_{xy} + B_{31}k_X^0 + B_{32}k_Y^0 + B_{33}k_{XY}^0 \\ M_X^0 = B_{11}\varepsilon_x^0 + B_{12}\varepsilon_y^0 + B_{13}\gamma_{xy} + D_{11}k_X^0 + D_{12}k_Y^0 + D_{13}k_{XY}^0 \\ M_Y^0 = B_{21}\varepsilon_x^0 + B_{22}\varepsilon_y^0 + B_{23}\gamma_{xy} + D_{21}k_X^0 + D_{22}k_Y^0 + D_{23}k_{XY}^0 \\ M_{XY}^0 = B_{31}\varepsilon_x^0 + B_{32}\varepsilon_y^0 + B_{33}\gamma_{xy} + D_{31}k_X^0 + D_{32}k_Y^0 + D_{33}k_{XY}^0 \end{cases}, \tag{5}$$

where

$N_X^0, N_Y^0, N_{XY}^0$ – forces that act per unit length of mid surface in direction X Y, XY;

$M_X^0, M_Y^0, M_{XY}^0$ – moments that act per unit length of mid surface in direction X Y, XY;

$A_{ij}, B_{ij}, D_{ij}$ – matrix coefficients that could be calculated according to eqs.(6).

$$\begin{aligned} A_{ij} &= \sum_{k=1}^{N}\left(\overline{Q_{ij}}\right)_k \left(z_k - z_{k-1}\right) \\ B_{ij} &= \frac{1}{2}\sum_{k=1}^{N}\left(\overline{Q_{ij}}\right)_k \left({z_k}^2 - {z_{k-1}}^2\right), \\ D_{ij} &= \frac{1}{3}\sum_{k=1}^{N}\left(\overline{Q_{ij}}\right)_k \left({z_k}^3 - {z_{k-1}}^3\right) \end{aligned} \tag{6}$$

where
*N*- number of layers;

$z_k, z_{k-1}$ – bottom and top coordinate on axis *Z* of layer number *k;*

$\bar{Q}_{ij}$ – matrix witch coefficient could be calculated according to eq. (7).

$$\begin{cases} \overline{Q}_{11} = C_1\left(E_1\cos^4\varphi + 2\left(E_1\nu_{21} + 2G_{12}(1-\nu_{12}\nu_{21})\right)\sin^2\varphi\cos^2\varphi + E_2\sin^4\varphi\right) \\ \overline{Q}_{22} = C_1\left(E_1\sin^4\varphi + 2\left(E_1\nu_{21} + 2G_{12}(1-\nu_{12}\nu_{21})\right)\sin^2\varphi\cos^2\varphi + E_2\cos^4\varphi\right) \\ \overline{Q}_{12} = C_1\left(\left(E_1 + E_2 - 4G_{12}(1-\nu_{12}\nu_{21})\right)\sin^2\varphi\cos^2\varphi + E_1\nu_{21}(\sin^4\varphi + \cos^4\varphi)\right) \\ \overline{Q}_{33} = C_1\left(\left(E_1 + E_2 - 2E_1\nu_{21} - 2G_{12}(1-\nu_{12}\nu_{21})\right)\sin^2\varphi\cos^2\varphi + G_{12}(\sin^4\varphi + \cos^4\varphi)\right) \\ \overline{Q}_{13} = C_1\left(\left(E_1 - E_1\nu_{21} - 2G_{12}(1-\nu_{12}\nu_{21})\right)\sin\varphi\cos^3\varphi + \left(E_1\nu_{21} - E_2 + 2G_{12}(1-\nu_{12}\nu_{21}\right)\sin^3\varphi\cos\varphi\right) \\ \overline{Q}_{23} = C_1\left(\left(E_1 - E_1\nu_{21} - 2G_{12}(1-\nu_{12}\nu_{21})\right)\sin^3\varphi\cos\varphi + \left(E_1\nu_{21} - E_2 + 2G_{12}(1-\nu_{12}\nu_{21}\right)\sin\varphi\cos^3\varphi\right) \end{cases} \tag{7}$$

where

$C_1 = \dfrac{1}{1-\nu_{12}\nu_{21}}$;

$\nu_{12}, \nu_{21}$ – Poisson’s ratio;

$E_1, E_2$ – Young’s modulus in axial direction of wood and in tangential direction of wood;

$G_{12}$ – shear modulus of wood in tangential - axial plane;

$\varphi$ – direction of fibres of each wood layer with axe *X*. Other coefficients of matrix $\overline{Q_{ij}}$ are obtained using symmetry.

In case of symmetrical structure of sheet and moisture distribution through the thickness of the sheet is uniform coefficients of matrix *A* and *D* are zeros (see eq.(6)) and values of curvatures and torsion are zero. If the moisture distribution through the thickness in not uniform but according to function $W(z)$, then coefficients of matrix *A* and *D* are not zeros because each layer has different elastic properties and curvatures and torsions of the sheet are not zero. Force and moment system that arise from moisture change and acts per unit length of sheet is calculated according to eq. (8).

$$\begin{aligned}\left[N_u^0\right] &= \sum_{k=1}^{N}\left[\overline{Q}_{ij}(W(z))\right]_k \left[\beta_u\right]_k (W_0 - W(z))(z_k - z_{k-1})\\ \left[M_u^0\right] &= \frac{1}{2}\sum_{k=1}^{N}\left[\overline{Q}_{ij}(W(z))\right]_k \left[\beta_u\right]_k (W_0 - W(z))({z_k}^2 - {z_{k-1}}^2)\end{aligned} \tag{8}$$

where

$W_0$ – value of initial moisture content of the sheet.

In the curvature analysis is assumed that in each layer the moisture distribution is uniform and its value is: $W\left(\dfrac{z_k + z_{k-1}}{2}\right)$.

*B. Large displacement analysis*

The strain- displacement relationship is obtained from Green-Lagrange strain tensor [10], using Kirchof-Love hypothesis of thin plates and assuming that in-plane displacement of the sheet is small:

$$\varepsilon = \begin{bmatrix} \dfrac{\partial u_1^0}{\partial x_1} - x_3\dfrac{\partial^2 u_3^0}{\partial x_1^2} + \dfrac{1}{2}\left(\dfrac{\partial u_3^0}{\partial x_1}\right)^2 \\ \dfrac{\partial u_2^0}{\partial x_2} - x_3\dfrac{\partial^2 u_3^0}{\partial x_2^2} + \dfrac{1}{2}\left(\dfrac{\partial u_3^0}{\partial x_2}\right)^2 \\ 0 \\ 0 \\ 0 \\ \dfrac{1}{2}\left(\dfrac{\partial u_1^0}{\partial x_2} + \dfrac{\partial u_2^0}{\partial x_1}\right) - x_3\dfrac{\partial^2 u_3^0}{\partial x_1 \partial x_2} + \dfrac{1}{2}\dfrac{\partial u_3^0}{\partial x_1}\cdot\dfrac{\partial u_3^0}{\partial x_2} \end{bmatrix} \tag{9}$$

The most convenient way of solving structural problems with geometrical non-linearity is Finite element method (FEM). Using the FEM for displacement analysis of multilayer sheet transverse displacements of mid-surface of sheet $u_3^0$ is approximated by appropriate polynomial (see eq.(10)). Order of polynomial depends on node count in element. Unknown coefficients of polynomial are solved using typical Finite element procedures [11].

$$u_3^0 = f\left(a_1, a_2, a_3, \ldots\right) \quad . \tag{10}$$

The unknown coefficients are obtained using minimum principle of minimum of total potential energy function:

$$\Pi = \sum_{i=1}^{N}\left[\frac{1}{2}\int_{x_3^{i-1}}^{x_3^{i}}\int_D \varepsilon^T \bar{Q}\,\varepsilon\, dA - \int_{x_3^{i-1}}^{x_3^{i}}\int_D \varepsilon^T \bar{Q}\,\varepsilon_w\, dA\right] \tag{11}$$

$$\begin{cases} \dfrac{\partial \Pi}{\partial a_1} = 0 \\ \dfrac{\partial \Pi}{\partial a_2} = 0\,, \\ \quad\ldots\ldots. \end{cases} \tag{12}$$

where

${\varepsilon_w}^T = \left[\alpha_{x1}\cdot\Delta W \quad \alpha_{x2}\cdot\Delta W \quad 0\right]$ are moisture caused stains;

$N$- total number of layers;

$x_3^i, x_3^{i-1}$ – i-th layer top and bottom coordinates in direction of sheets thickness;

$\alpha_{x1}, \alpha_{x2}$ – material expansion coefficients when moisture varies 1 %.

The nonlinear algebraic system of equation (12) could be solved by using Newton-Rapson iteration method [10]. The Finite element method (FEM) gives accurate results if mesh is smooth enough. FEM is inconvenient if it is necessary to do displacement analysis for great number of cases. Therefore further the shape analysis of multilayer sheet is done by using simplified method produced by authors [12]-[14], combined with previously described equations. This method is based on following relationship:

$$\begin{bmatrix} k_X^0(w) \\ k_Y^0(w) \end{bmatrix} = \sum_{l=1}^{n} \begin{bmatrix} k_X^0(w) \cdot \dfrac{I_{0,y}}{I_{l,y}} \\ k_Y^0(w) \cdot \dfrac{I_{0,x}}{I_{l,x}} \end{bmatrix}_l , \quad (13)$$

where

.

$I_{0,x}, I_{0,y}$ – moment of inertia for flat plate relative to axis x and y;

$I_{l,x}, I_{l,y}$ – moment of inertia for *l* step curved plate relative to axis *x* and *y*;

n- total number of iteration.

It is necessary to take into account the geometrical nonlinearity of the sheet with orthogonal structure if difference between moments of inertia for a flat sheet and curved sheet is greater than 5% [13].

## IV. RESULTS OF ANALYSIS OF MOISTURE DISTRIBUTION

Moisture distribution through the thickness of the sheet is analysed according to equation (1). The sheet consists of 9 birch layers; its total thickness is 13.5mm. Assumed that surface emission coefficient is not dependent on moisture content and temperature. In the first case the initial moisture level through the thickness of the sheet is 12% and from one side of the sheet the relative humidity (*RH*) of air is 65% ( wood moisture *W*=13% according to [3]) form other side *RH*=53% (*W*=10% according to [3]). Temperature is constant 293.15 K. The obtained results at discrete time are shown in fig. 2

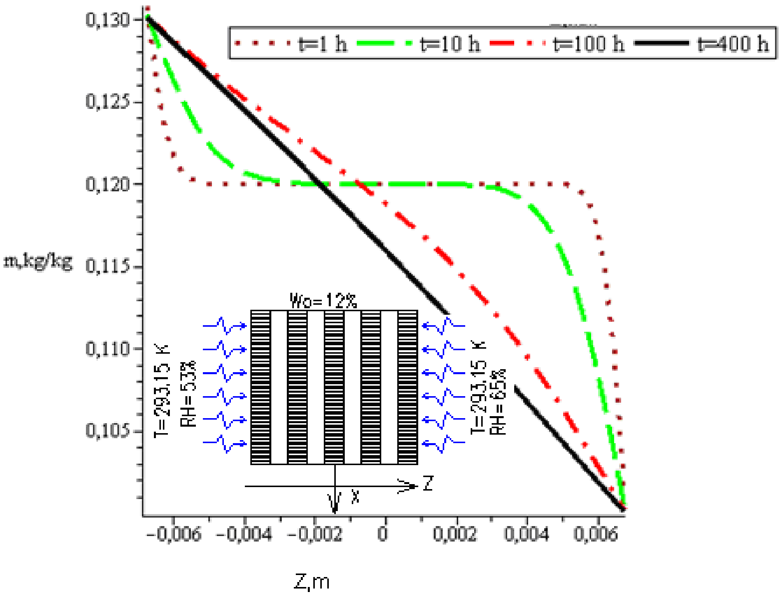

Fig. 2. The distribution of moisture content through the thickness of sheet at varying time periods

Another case was analysed for moisture distribution through the thickness of sheet. The initial moisture content of wood is 12% and from one side relative humidity of air is *RH*=56% and temperature *T*=293 *K*. For this environment conditions wood moisture content is about 11% [3]. Other side is covered with moisture isolation. The results are shown in Fig.3.

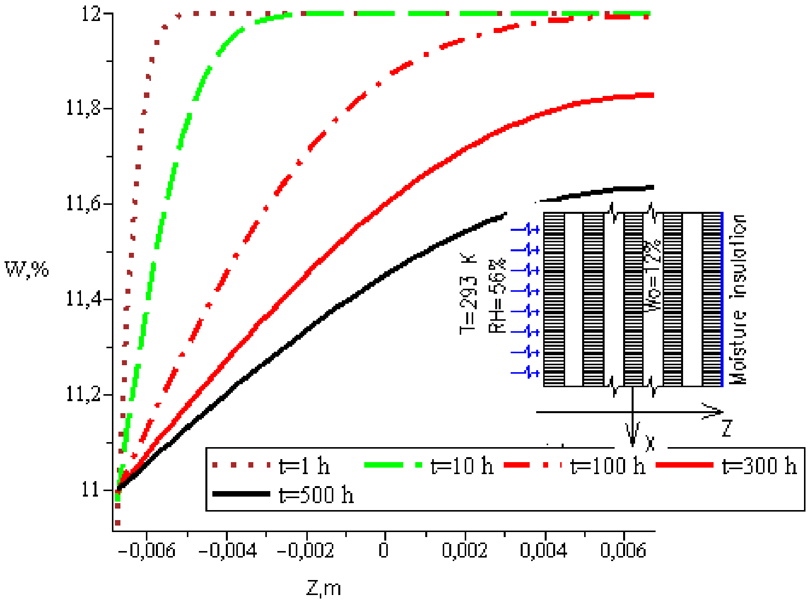

Fig. 3. The distribution of concentration of moisture through the thickness of sheet after varying time periods (*t*- time).

The moisture diffusion theoretical analysis was verified by experimental results taken form literature [15]. The sheet consists of 7-veneer structure. The first and 7th veneer is made from modified wood with density 900 kg/m3, after gluing process. The thickness of top and bottom veneer are 1.5 mm. Thickness of all other veneers are 2 mm. Total thickness of the sheet is 13mm. Veneers are modelled like orthotropic material and mechanical properties of layers are obtained from literature [15]. The initial moisture content of the sheet is 6.5%. One side of sheet is above opened water source with distance from it 50mm. Other side of the sheet is subjected to normal indoor air conditions- temperature 293 K and relative humidity 60%. The results in experimental and theoretical analysis are shown in Fig. 4. It shows that theoretically obtained results are in good agreement with experimental results. Experimental results are with 95% statistical guarantee.

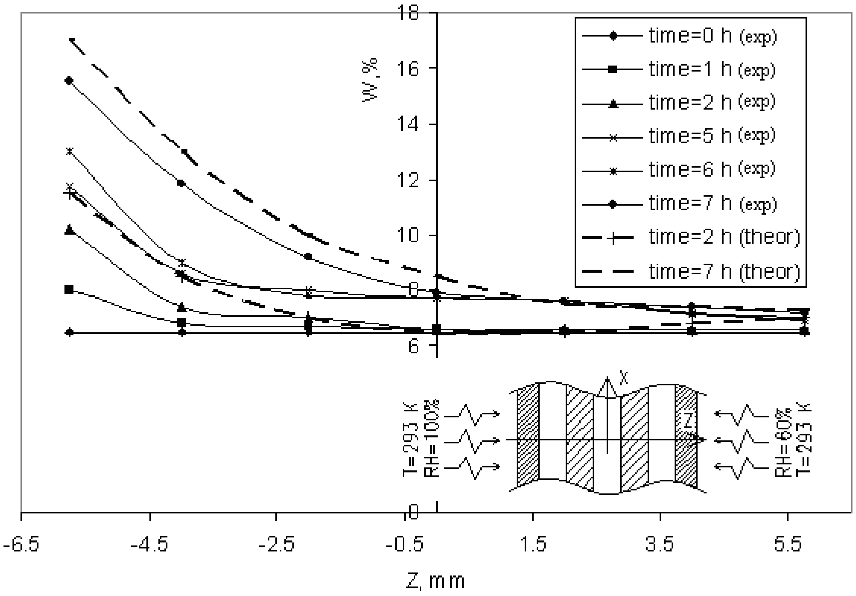

Fig. 4. Experimentally and theoretically obtained moisture distribution through thickness of sheet

## V. RESULTS OF CURVATURE ANALYSIS

### *A. Curvature analysis of sheet in non-time-dependent environment conditions*

Analysis of curvature was done for a few cases of moisture-temperature conditions. The curvature was calculated for the sheet showed in fig.5. The sheet consists of nine birch veneers. Wood fibre direction of five layers is parallel to *Y* axis and others are parallel to *X* axis. Total thickness of the sheet is 13.5 mm. Sheet is square shaped and length of edge – 1500 mm.

The following elastic characteristics for birch layers were used in analysis [16]:

$$E_a(12\%) = 16400MPa$$
$$E_t(12\%) = 530MPa$$
$$G_{ta}(12\%) = 890MPa$$
$$v_{at} = 0.04$$
$$v_{ta} = 0.45$$

*a*- axial direction of wood fibre;
*t*- tangential direction of wood fibre.

The values of elastic characteristic when moisture content is below FSP could be calculated by following equations [16]:

$$\begin{aligned} E_a(W) &= E_a(12\%) - 200\cdot(W-12) \\ E_t(W) &= E_t(12\%) - 25\cdot(W-12) \\ G_{ta}(W) &= G_{ta}(12\%) - 30\cdot(W-12) \end{aligned} \tag{14}$$

where

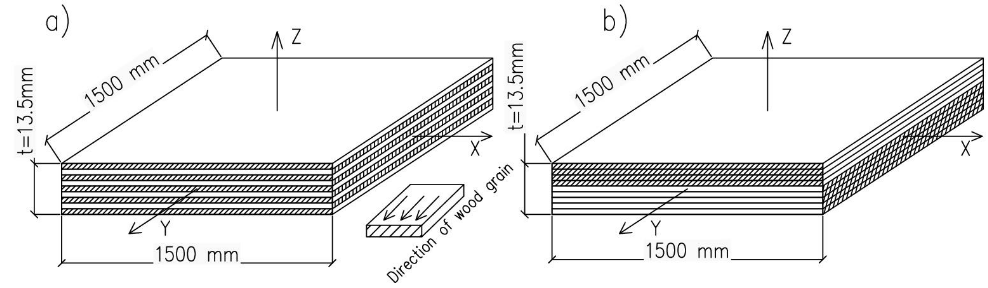

Fig. 5. Structure and dimensions of the sheet: a- sheet with symmetrical- orthogonal structure, b- sheet with asymmetrical- orthogonal structure.

Values of curvature analysed according to initial and boundary conditions shown in Fig. 2. In case if the sheet is with symmetrical-orthogonal structure (see fig. 5.a) curvature analysis results are shown in Fig. 6.

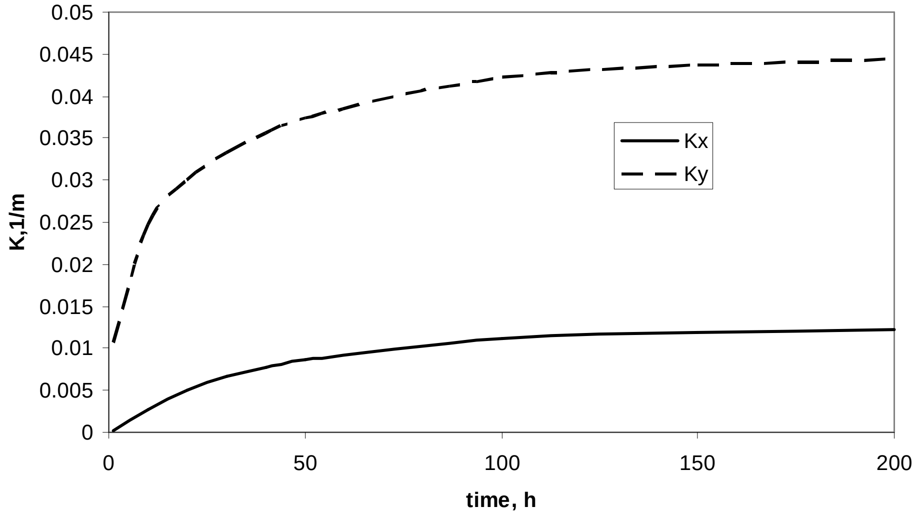

Fig. 6. Values of curvatures depending on time according to moisture distribution shown in Fig. 2. for the sheet with structure shown in Fig.5.a.

Values of curvature is analysed according to initial and boundary conditions shown in Fig. 2. In case if the sheet is with asymmetrical - orthogonal structure (see fig. 5.b) obtained results are shown in Fig. 7.

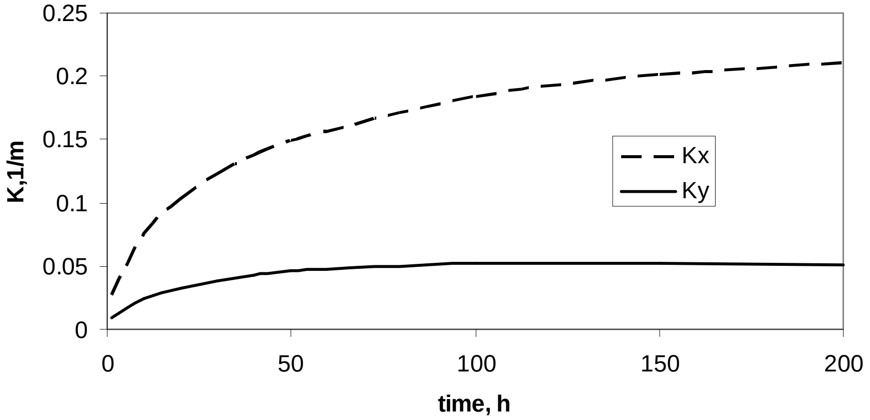

Fig. 7. Values of curvatures depending on time according to moisture distribution shown in Fig. 2. for a sheet with structure shown in Fig.5.b

Values of curvature calculated according to initial and boundary conditions shown in Fig. 3. In the case if the sheet is with asymmetrical- orthogonal structure (see fig. 5.b) results are shown in Fig. 8.

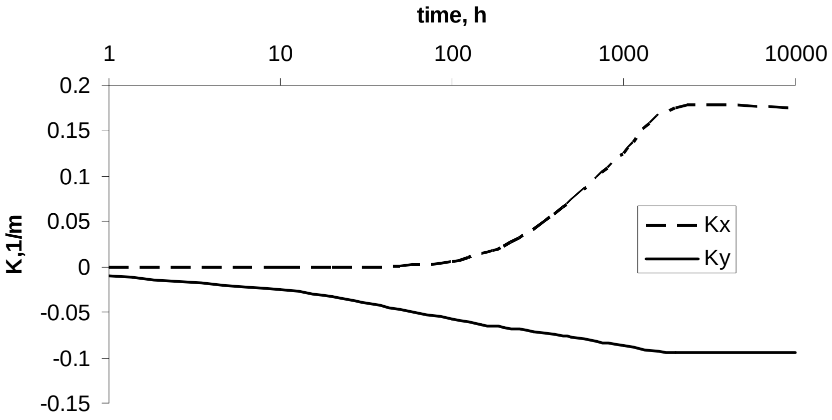

Fig. 8. Values of curvatures depending on time according to moisture distribution shown in Fig.3 for a sheet with structure shown in Fig.5.b.

The analysis of curvature was verified by experimental data that is obtained from literature [15]. Curvature analysis was done for the square shaped sheet with length of edge equal to 480mm and total thickness 13mm. The sheet has 7-layer structure. Outside layers are made from modified alder wood, that has density about 900 kg/m$^3$ after gluing process. Other five layers are made from non-modified alder wood. The thickness of first and last layer is 1.5mm thickness other layers is 2mm. The initial moisture content of the sheet is 6.5 %. The curvature analysis is done at discrete time according to moisture distribution curves shown in Fig. 4.

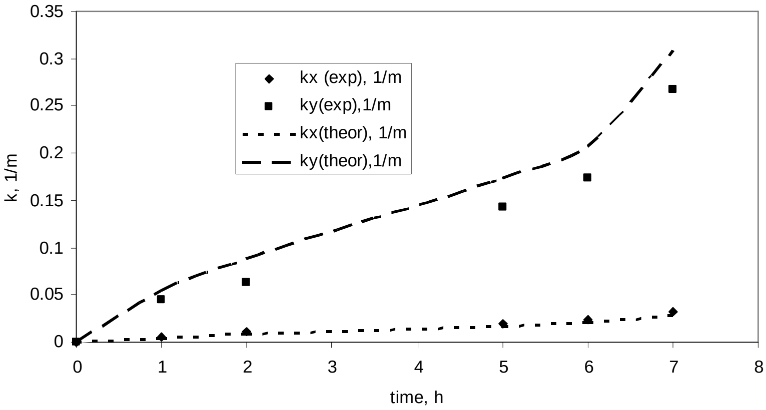

Fig. 9. Experimentally and theoretically obtained curvatures for 7-layer sheet according to [15] with 95% statistical guarantee.

.

### *B. Curvature analysis of sheet in time-dependent environment conditions*

Another numerical experiment was done to simulate the behaviour of the sheet that is shown in Fig.4.a for the case when one side of the sheet is subjected to outdoor conditions and other side of the sheet is in indoor conditions - *T*=293.3 K, RH=50%. The maximal outdoor relative humidity (sum of average humidity and its amplitude) and average temperature are taken from national standard LBN-003-01 "Būvklimatoloģija" for the Riga. In the calculation relative humidity (*RH*) and temperature of the outside are approximated by third order polynomial:

$$RH = 0.877 + 0.000587t + 4.46 \cdot 10^{-6} t^2 - 1.79 \cdot 10^{-8} t^3 \tag{15}$$

$$T = -9.418 + 0.146 \cdot t + 0.000236 \cdot t^2 - 1.8 * 10^{-6} \cdot t^3 \tag{16}$$

where

*t*- time in days (*t*=0- first January, *t*=365- 31. December); *T*- temperature in (K);

*RH*- relative humidity (%).

The moisture content of birch wood could be approximated by following equation depending on relative humidity of air and temperature [3]:

$$m(\varphi, T) = 0.0638 + 0.1096 \cdot RH + 0.0001947 \cdot T + 0.1219 \cdot RH^2 - 9.8 \cdot 10^{-7} \cdot T^2 - 0.00017 \cdot RH \cdot T . \tag{17}$$

Moisture distribution curves through the thickness of sheet at discrete time are shown in Fig. 10. Offset of moisture distribution curve at the time about 50 week could be explained by smallest average relative humidity of air in the winter months (December- January). The results of curvature analysis in different month are shown in Fig. 11.

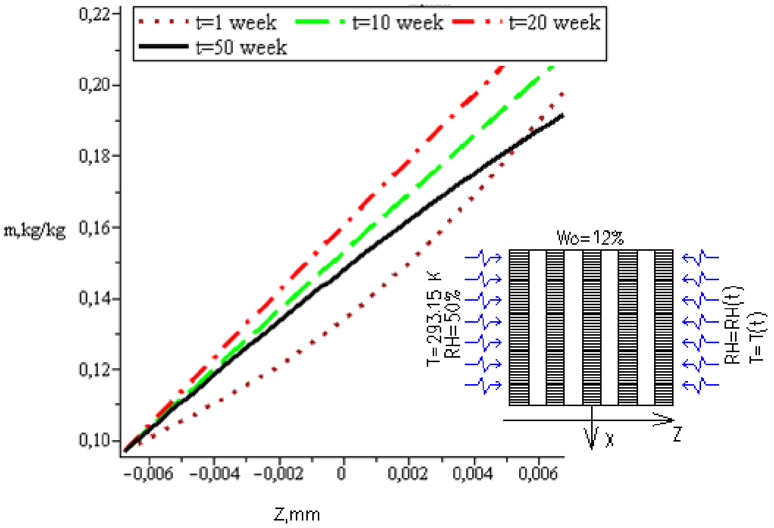

Fig. 10. Moisture distribution through the thickness of sheet at varying time.

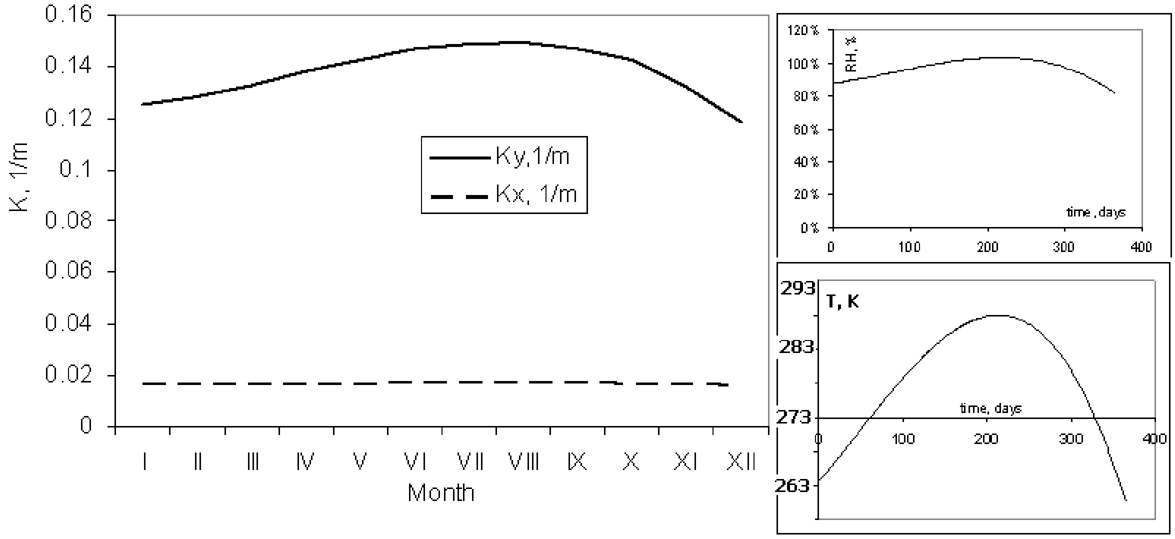

Fig. 11. The average values of curvature depending on month for a sheet with structure shown in Fig. 5.a.

## CONCLUSIONS

Numerical analysis of moisture diffusion process in plywood sheet is done and moisture distribution curves through thickness of the sheet when there are different moisture conditions in each side of the sheet are obtained.

Values of curvature of the sheet with symmetrical - orthogonal structure and asymmetrical - orthogonal structure with respect to sheet mid-surface were calculated for a various moisture distribution curves through the thickness of the sheet. The sheet obtains maximal curvature when equilibrium state in moisture diffusion process occurs. Time–dependent numerical curvature analysis of 7-layer sheet conformed to experimental results.

Calculated values of curvature when one side of sheet is subjected outdoor time-dependent temperature-moisture conditions where average relative humidity (summed with average amplitude) and average temperature of air throughout the astronomic year in Riga are approximated using polynomials. Maximal displacements of the sheet occur at the middle of summer.

## REFERENCES

1. **Avramidis, S., Englezos, P., Papathanasiou, T.** Dynamic nonisothermal transport in hygroscopic porous media: moisture diffusion in wood. *AIChE J.*, 1992, Vol. 38, p. 1279–1287.
2. **Pang, S.** Relationship between a diffusion model and a transport model for softwood drying. *Wood Fiber Sci.*, U.K, 1997, Vol. 29, p. 58–67.
3. **Шубин, Г. С.** *Физические основы и расчет процессов сушки древесины*. Москва: Лесная промишленность, 1973. 248 с.
4. **Liping, C.** Determination of diffusion coefficients for sub-alpine fir. *Wood science and technology*, U.K., 2005, Vol. 39, p. 153-162.
5. **Wieslav, O., Jerzy, W.** Effects of the method of identification of the diffusion coefficient on accuracy of modeling bound water transfer in wood. *Transport in porous media*, London, 2007, Vol. 66, p. 135-144.
6. **Wook, K., Woo, Y. C., Chang, D. E., and others**. Some considerations in heterogeneous nonisothermal transport models for wood: a numerical study. *Journal of Wood Science,* London, 2008, Vol. 54, p. 267-277.
7. **Reissner, E., Stavsky, I.** Bending and stretching of certain types of heterogeneous aleotropic elastic plates. *Trans. ASME*, Ser. E, 1961, Vol. 28, N 3, p. 402-408.
8. **Rocens, K., Steiners, K.** Stiffness and ductability analysis for unbalanced monoclinic composite. *Mechanic of polymer*, Riga, 1976, Vol. 6, p.1030-1035.
9. **Skudra, A.M., Skudra, A.A.** *Ievads slāņaino materiālu mehānikā.* Riga: RTU, 2002. p. 116.
10. **Bonet, J., Wood, R.D.** *Nonlinear continuum mechanics for finite element analysis*. UK: Cambridge university press, 1997. p. 283.
11. **Zienkiewicz, O.C., Taylor, R.L.** *The Finite Element Method. Vol. 2. Solid Mechanics*. London: McGraw-Hill, 2000. p. 459.
12. **Sliseris, J., Rocens, K.** Curvature analysis for asymetical multi-layer composite. *Construction Science*, Riga, RTU, 2009, Vol. 10, N 2, 2010, p.140–148.
13. **Sliseris, J, Rocens, K.** Curvature Analysis for Composite with Orthogonal, Asymmetrical Multi-Layer Structure. *Journal of Civil Engineering and Management*, Vol. 16, N 2, 2010, pp. 242-248.
14. **Sliseris, J., Rocens, K.** Behaviour of multilayer sheet with technogical imperfection. ***In**: 1oth International Conference „Modern Building Materials, Structures and Techniques”*, Lithuania, 2010, pp. 793-798.
15. **Роценс, К. А.** Технологическое регулирование свойств древесины. Рига: Зинатне, 1979. 222 с.
16. **Перелыгин, А. М., Уголев, Б. Н.** *Древесиноведение*. Москва,: Лесная промышленность, 1971, 286 с.

**Jānis Šliseris** is a scientific assistant and PhD student of structural engineering at the Riga Technical University, Latvia. He is a and participant from Latvia in COST C25 ”Sustainability of Constructions: Integrated Approach to Life Time Structural Engineering”. He is author of 3 scientific articles. His research interests include the modern structures, numerical simulation of structures, moisture diffusion problems in wood and wood based composites, technological mechanics of wood and composite materials.
Address: 1 Kalķu Street, Riga LV-1658
E-mail: janis.sliseris@gmail.com

**Kārlis Rocēns** is a professor of structural engineering and director of the Institute of Structural Engineering and reconstruction at the Riga Technical University, Latvia. He is a Full member of Latvian academy of sciences and participant from Latvia in COST C25 ”Sustainability of Constructions: Integrated Approach to Life Time Structural Engineering”. He is author of 5 monographs and more than 250 scientific articles. His research interests include the modern structures, technological mechanics of wood and composite materials and structural material science.
Address: 1 Kalķu Street, Riga LV-1658, Latvia, E-mail: rocensk@latnet.lv

**Jānis Šliseris, Kārlis Rocēns. Mainīga mitruma ietekme uz slāņainas koksnes materiālu formu**

Noteikts mitruma saturs pa saplākšņa loksnes biezumu pie atšķirīga mitruma loksnes abās pusēs, risinot difūzijas vienādojumu. Aprēķinā apskatīti gadījumi, kad loksnei abās pusēs ir nemainīgi mitruma režīmi un vienmērīga temperatūra, kā arī gadījums, kad loksnei viena puse ir tiešā saskarē ar ārtelpu, līdz ar to mainīgu temperatūras-mitruma režīmu, šis režīms noteikts kā vidējais temperatūras un vidējā gaisa mitrums, kam pieskaitīta vidējā mitruma amplitūda pēc būvnormatīva LBN-003-01 "Būvklimatoloģija", approksimējot vidējās vērtības ar trešās pakāpes polinomu, otra loksnes puse atrodas apkurināmā telpā ar nemainīgu temperatūras-mitruma režīmu.

Teorētiski aprēķinātais mitruma sadalījums pa 7-slāņu loksnes biezumu ir ļoti tuvs eksperimentāli iegūtajam. Liekumu vērtības, kas atrastas eksperimentāli, ir tuvas teorētiski aprēķinātajām vērtībām.

Izmantojot iegūto mitruma sadalījumu pa loksnes biezumu, noteikti loksnes liekumi, kad loksnei ir simetriski ortogonāla struktūra un kad tai ir nesimetriski ortogonāla struktūra. Loksne ar simetriski ortogonālu struktūru, mainoties mitrumam pa tās biezumu, var iegūt pozitīvu vai nulles Gausa liekumu, taču loksne ar nesimetriski ortogonālu struktūru var iegūt pozitīvu, negatīvu un nulles Gausa liekumu. Loksne maksimāli pārveidojas, kad iestājies mitruma maiņas līdzsvars pa tās biezumu. Loksne, kas no vienas puses pakļauta apkārtējās vides mainīgajam temperatūras un mitruma režīmam, un no otras puses – telpas temperatūrai un iekšējam mitrumam, satur 12% mitruma, maksimālie pārveidojumi un izliekumi notiek vasaras mēnešos.

**Янис Шлисерис, Карлис Роценс. Влияние изменения влаги на форму слоистых древесных материалов**

Путём решения диффузионных уравнений для одноосного случая определяется распределение влаги по толщине листа во времени. При расчете рассматриваються случаи, когда по обеим сторонам листа влажность и температура постоянны, а также случий, когда одна сторона листа находится в контакте с окружающей средой, т.е. изменяется во времени влажность и температура, с учётом строительных норм LBN-003-01 „Būvklimatoloģija", а вторая сторона листа находится в помещении с постоянным режимом влажности и температуры.

Рассчитанные распределения влажности через толщину 7-слойного листа подтверждается экспериментальными данными. Величины изгиба, которые определены экспериментально, практически подтверждает рассчитанные величины.

Используя полученные распределения влажности по толщине листа, определены изгибы листа, в случаях когда пластина имеет симетрично-ортогональную структуру и когда она имеет несиметрично-ортогональную структуру. Листы с симетрично-ортогональной структурой в процессе изменения влажности могут получить позитивный или нулевой выгиб Гауса, но листы с несиметрично- ортогональной структурой могут получить позитивный, негативный и нулевой выгиб Гауса. Максимальные перемещения пластина достигает в тех случаях, когда наступает равновесие влажности листа с влажностью окружающей среды. Установлено, что пластина с 12%-ным содержанием влаги, которая с одной стороны подвергнута действию температуры и влажности окружающей среды а с другой- постоянной влажности и температуры помещения, максимальные перемещения и изгибы достигает в летние месяцы года.